Seismic Behavior of Tunnel Form Building under Lateral Cyclic Loading

Nor Hayati Abdul Hamid[1*], Shamilar Anuar[2], Haryati Awang[3] & Mahmud Kori Effendi[4]

[1]Institute for Infrastructure Engineering, Sustainability and Management (IIESM), Universiti Teknologi MARA, 40450 Shah Alam, Selangor, Malaysia
[2]School of Environmental Engineering, Universiti Malaysia Perlis, Kompleks Pusat Pengajian Jejawi 302600, Arau, Perlis, Malaysia
[3]Faculty of Civil and Earth Resources, Universiti Malaysia Pahang, 26300, Gambang, Kuantan, Pahang, Malaysia
[4]Fakultas Teknikal Sipil, Universitas Negeri Semarang, Jalan Sekaran, Gunung Pati, Kota Semarang, Jawa Tengah, 50229, Indonesia
*E-mail: norhayati4837@yahoo.com

Abstract. A three-story single-unit tunnel form building (TFB) was designed using a non-seismic code of practice (BS 8110). Two one-third scale test models were constructed and tested under in-plane lateral cyclic loading and out-of-plane lateral cyclic loading, respectively. The specimens were tested at ±0.01%, ±0.1%, ±0.25%, ±0.5%, ±0.75%, ±1.0%, ±1.25%, ±1.5%, ±1.75% ±1.8, ±1.9% and ±2% drifts, after which severe cracks were observed on the wall-slab joints and wall panels. Subsequently, the damaged specimens were repaired and retrofitted by wrapping carbon fiber reinforced polymer (CFRP) around the damaged walls and affixing steel plates and steel angles at the wall-slab joints using several different repair and retrofitting schemes. The repaired specimens were retested using the same drifts. The comparison of the seismic behavior between unrepaired and repaired specimens was made based on visual observation of damage, hysteresis loops, lateral strength capacity, stiffness, ductility, and equivalent viscous damping. The experimental results showed that the repaired specimens were improved in terms of damage, lateral strength capacity, stiffness, ductility, and equivalent viscous damping. It is recommended to strengthen and rehabilitate tunnel form buildings after an earthquake using CFRP, additional shear walls, steel plates and steel angles.

Keywords: *damaged specimens; ductility; equivalent viscous damping; rehabilitation; stiffness.*

1 Introduction

To date, few studies have been conducted to determine the seismic performance of tunnel form building systems under in-plane and out-of-plane lateral cyclic loading [1-4]. Moreover, in these studies no repair or retrofitting schemes were carried out for tunnel form buildings. It is evident that the poor seismic behavior of these types of buildings during the 1999 Kocaeli Earthquake and the 1999 Duzce Earthquake in Turkey caused severe damages. These buildings had to be

Received August 28th, 2017, Revised April 9th, 2018, Accepted for publication June 5th, 2018.
 ISSN: 2337-5779, DOI: 10.5614/j.eng.technol.sci.2018.50.2.5

repaired and strengthened before they could be occupied again after the earthquake.

Common problems encountered with shear walls in tunnel form buildings are that they have inadequate strength to resist lateral forces and transfer them to the foundation of the building due to the absence of diagonal bracing on the shear walls. An effective way of repairing them is to wrap the damaged structural components with carbon fiber reinforced polymer (CFRP) perpendicular to potential shear cracks. Three repairing techniques using CFRP, i.e. full wrapping, three-sided wrapping (U-shape) and two-sided wrapping, have been investigated to determine the best technique [5-7]. If the bond zone between the wrapping surface and the CFRP fabric is larger, then the lateral strength capacity of the structure will increase gradually. Furthermore, another research revealed that the use of FRP sheets wrapping the wall surface increased its displacement ductility by 57% when compared to the control wall [8-10]. Layssi has studied the poor seismic response of shear walls and then repaired and retrofitted damaged walls using CFRP fabrics [11-13]. Others studies on shear walls and precast walls have been conducted in order to determine the seismic behavior of low-ductility precast walls under in-plane lateral cyclic loading [14-17]. Recently, strengthening techniques for non-ductile reinforced concrete shear walls using externally bonded CFRP sheets under in-plane seismic loading have been investigated [18,19]. There are also several seismic retrofitting schemes for repairing local and global damage to reinforced concrete structures caused by earthquake disasters [20-22]. Based on past research work on repair and retrofitting schemes for shear walls, the most effective technique is fully wrapping the whole damaged shear wall panel with CFRP. Hence, this technique was adopted in this study.

2 Design and Construction of Tunnel Form Building

In this study, a tunnel form building was designed using British Standard 8110 [23], which is a non-seismic code of practice that has no provision for earthquake resistance. This building was designed to carry a vertical load that only consists of dead load and imposed load with a safety factor of 1.4 and 1.6, respectively. However, according to British Standard 8110 Part 2, the notional horizontal load that applies to each floor level is 1.5% of the characteristic dead weight of the structure. Unfortunately, this notional lateral load is very small compared to the lateral load caused by moderate to strong earthquakes. The design processes of the tunnel form building was aimed at determining the design load (w_d), designing the shear walls of the tunnel form building, designing the flat slab, and finally designing the foundation beam. The number of reinforcement bars in the shear wall was determined by dividing the axial load with the yield stress of steel. The thickness of the steel plate and steel angle

depends on the bending moment at the wall-slab joints. The compressive strength of concrete for shear walls is 35 N/mm^2 and the tensile strength of steel is 460 N/mm^2. Initially, the tunnel form building behaves linearly, until it reaches the yield load, followed by nonlinear behavior starting from yield load, up to failure load. Due to space limitations, the actual building was scaled down to one-third scale for use as the test model.

Figure 1 shows a front view of the design detailing of the reinforcement bars of the three-story single-unit TFB, with diameters of 6 mm, 10 mm and 16 mm for the bars. Meanwhile, Figure 2 shows a side view of the detailing of the reinforcement bars of the three-story TFB using a diameter of 6 mm for the shear walls and 16 mm for the reinforcement bars of the foundation beam. Construction involved two phases and took place at the Heavy Structural Laboratory, Faculty of Civil Engineering, Universiti Teknologi MARA, Shah Alam, Selangor, Malaysia. The first phase involved the construction of two single units of a TFB and included the preparation of the reinforcement bars, the cages for the foundation beam, the formwork for wall panels and slabs, the pouring of wet concrete into the formwork and the curing of the specimens at ambient temperature. The second phase was the experimental set-up, calibration of the instruments, testing of the specimens, repairing and retesting of the specimens using the same loading regime under in-plane and lateral cyclic loading. Figure 3 shows the one-third scale three-story single-unit of the TFB test model ready to be tested under in-plane lateral cyclic loading, where two holes at the top of the specimen were used to clamp the specimen to a double actuator. Meanwhile, the second TFB model, which was to be tested under out-of-plane lateral cyclic loading, had four holes on top.

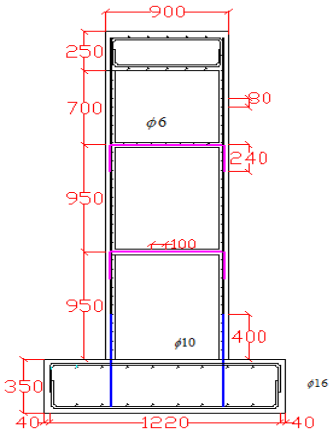

Figure 1 Front view of details of reinforcement bars in TFB.

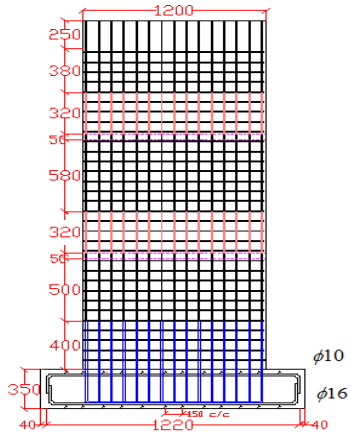

Figure 2 Side view of details of reinforcement bars for TFB.

Figure 3 Isometric view of TFB model ready for experimental testing.

3 Repair and Retrofitting Schemes

After the two specimens were tested under in-plane and out-of-plane lateral cyclic loading, respectively, the specimens were repaired and retrofitted using different repair and retrofitting schemes depending on the severity of the damage. The first TFB specimen, which had been tested previously under in-plane lateral cyclic loading, was repaired and retrofitted using CFRP, with a steel plate and a steel angle. Figure 4 shows the process of repairing and retrofitting the TFB specimen by affixing the steel plate and the steel angle at the wall-slab joint and then wrapping the whole shear wall with CFRP. The characteristic tensile strength of CFRP is 2800 MPa, the Young modulus E = 165 kN/mm^2, and density is 1600 kg/m^3. The second specimen, which had been tested under out-of-plane lateral cyclic loading and had suffered severe damage at the wall-slab joints, was repaired using a steel plate and a steel angle. Then, this specimen was re-tested using the same loading pattern before repairing it, until more cracks were observed at the outer and inner wall. Finally, the damaged wall panel was repaired again using CFRP fabric, and retested for a third time. A comparison was made between the unrepaired and repaired specimen based on visual observation damage, hysteresis loops, stiffness, ductility, and energy dissipation. Table 1 shows the amount of drift imposed on the unrepaired and repaired test models under in-plane and out-of-plane lateral cyclic loading.

Table 1 Drift Percentage Imposed on Specimens

Specimen	Drift percentage
S-INP-BR	±0.01%, ±0.1%, ±0.25%, ±0.5%, ±0.75%
S-INP-AR (SP + SA+CFRP)	±0.01%, ±0.1%, ±0.25%, ±0.5%, ±0.75%, ±1.0%, ±1.25%, ±1.5%
S-OUT-BR	±0.01%, ±0.1%, ±0.25%, ±0.5%, ±0.75%, ±1.0%, ±1.25%, ±1.5%, ±1.75%
S-OUT-AR (SP + SA + CFRP)	±0.01%, ±0.1%, ±0.25%, ±0.5%, ±0.75%, ±1.0%, ±1.25%, ±1.5%, ±1.75% ±1.8, ±1.9%, ±2%

Figure 4 Repair and retrofitting process of test model using CFRP fabric.

4 Experimental Results and Data Analysis

The experimental results and data analysis for all three specimens were compared based on visual observations of damage, hysteresis loops, lateral strength capacity, stiffness, ductility and equivalent viscous damping. The best repair and retrofitting scheme will be recommended based on the comparisons made between the unrepaired and the repaired specimens.

4.1 Comparison of Unrepaired and Repaired Test Model Under In-Plane Lateral Cyclic Loading

Figure 5 shows a comparison of the visually observed damage for the unrepaired test model and the same model that was repaired using a steel angle, a steel plate and CFRP fabric subjected to in-plane lateral cyclic loading only. It can be seen that the unrepaired specimen, labeled S-INP-BR, had some horizontal hairline cracks on the inner and outer surfaces of both walls at the first and second floor level at ±0.75% drift, as shown in Figure 5(a) and Figure 5(c), respectively. In contrast, no horizontal cracks were observed on the inner and outer sides of both walls at the first and second floor of the wall for the S-

INP-AR (SA+SP+CFRP) specimen at ±0.75% drift, as shown in Figure 5(b) and Figure 5(d), respectively.

S-INP-BR

(a) Horizontal cracks at ±0.75% drift.

S-INP-AR(SA+SP+CFRP)

(b) No cracks observed at ±0.75% drift

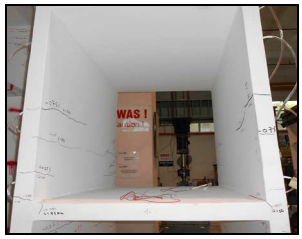

(c) Horizontal cracks at ±0.75% drift

(d) No cracks observed at ±0.75% drift

Figure 5 Comparison of visual observation of damages of unrepaired and repaired TFB specimens.

Figure 6 shows a comparison of the hysteresis loops between the unrepaired and repaired specimens based on the measurement of load versus displacement obtained at LVDT1 at the top part of the test model. The ultimate in-plane load for the S-INP-BR specimen was 42kN and 45kN for the S-INP-AR(SA+SP+CFRP) specimen at +0.75% drift. It can also be observed that the area of the hysteresis loops was higher for the repaired specimen than for the unrepaired specimen. This means that the repaired specimen could absorb more seismic energy and better protect the wall from damage and collapse.

Stiffness is the rigidity of the structure, where the extent to which it can resist deformation in response to an applied force under linear and nonlinear limits is known as elastic stiffness (K_e) and secant stiffness (K_{sec}), respectively. The formulas to calculate the elastic stiffness and secant stiffness are as follows:

$$K_e = \frac{F_y}{\Delta_y} \tag{1}$$

$$K_{sec} = \frac{F_{ult} - F_y}{\Delta_{ult} - \Delta_y} \tag{2}$$

where F_y= yield lateral load, Δ_y= yield lateral displacement, F_{ult} = ultimate lateral displacement and Δ_{ult}= ultimate lateral load. From Table 2, the maximum value of elastic stiffness (K_e = 9.5) for the unrepaired specimen, which occurred in the pushing direction in the first cycle, was higher than for the repaired specimen (K_e = 8.06) in the second cycle. Meanwhile, the maximum value for secant stiffness (K_{sec} = 1.95) for the repaired specimen was higher than for the unrepaired specimen (K_{sec} = 1.08). Therefore, it can be concluded that the elastic stiffness before repair was higher than for the repaired specimen and the secant stiffness was higher for the repaired specimen than for the repaired specimen. This is supported by results obtained from experimental work on an exterior beam-column joint with and without steel fibred reinforced concrete [24].

Table 2 Values of K_e and K_{sec} for unrepaired and repaired specimens under in-plane lateral cyclic loading.

Stiffness (kN/mm)	Before repair	After repair	Difference percentage
K_e	9.5	7.85	17.36%
K_{sec}	1.08	1.61	49.07%
(a) Pushing load in the first cycle			
Stiffness (kN/mm)	**Before repair**	**After repair**	**Difference percentage**
K_e	9.02	8.06	10.64%
K_{sec}	1.72	1.95	13.37%
(b) Pushing load in the second cycle			

S-INP-BR S-INP-AR(SA+SP+CFRP)

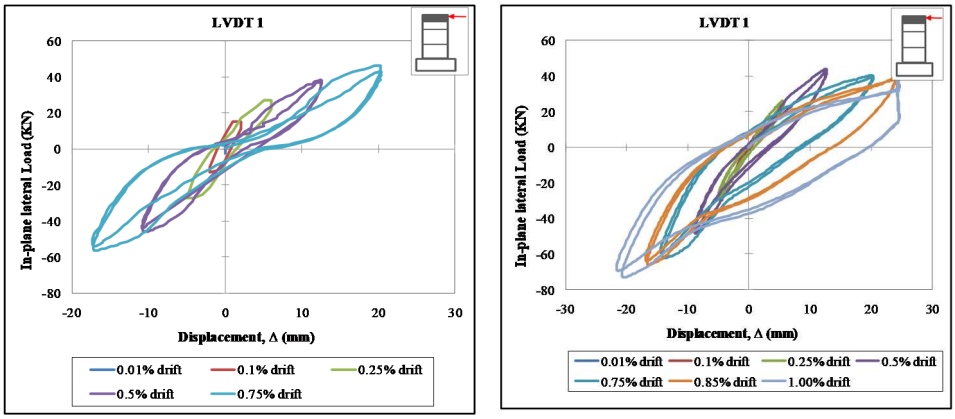

(a) Hysteresis loops of LVDT1 (b) Hysteresis loops of LVDT1

Figure 6 Comparison of hysteresis loops between unrepaired and repaired specimens.

Ductility is the ability of a structure to undergo permanent deformation through elongation under lateral cyclic loading. The formula used to calculate the ductility of the unrepaired and repaired specimens is in Eq. (3) as follows [25]:

$$\mu_{\Delta} = \frac{\Delta_{ult}}{\Delta_{y}} \tag{3}$$

Table 3 shows a comparison of displacement ductility between the unrepaired specimen and the repaired specimen, both tested under in-plane lateral cyclic loading. The maximum value of displacement ductility (μ_{Δ}) occurred in the repaired specimen with a value that was 1.50 higher than in the unrepaired specimen. It can be concluded that the steel plate, the steel angle and the CFRP increased the secant stiffness and ductility of the repaired specimen significantly when compared to the unrepaired specimen. A similar study showed that these materials could increase the seismic performance of a beam-column joint [26].

Table 3 Comparison of μ_{Δ} between unrepaired and repaired specimens.

Cycle	Direction	Displacement ductility (μ_{Δ})		Difference percentage
		Before repair	After repair	
First cycle	Pushing	1.14	1.21	6.14%
	Pulling	1.00	1.47	47.00%
Second cycle	Pushing	1.00	1.21	21.00%
	Pulling	1.00	1.50	50.00%

The equivalent viscous damping concept was first introduced by Jacobsen in 1930 [27]. In his paper, Jacobsen approximated the steady state solution of a nonlinear SDOF system by equating the energy dissipated by that system to the energy dissipated by one cycle of sinusoidal response of a linear system. However, the most common method for defining equivalent viscous damping is to equate the energy dissipated in a vibration cycle of an inelastic system and of an equivalent linear system. Based on this concept, it can be shown that the equivalent viscous damping ratio can be calculated using Eq. (4), derived from [28]:

$$\varepsilon_{eq} = \frac{1}{4\pi}\frac{E_D}{E_{so}} \tag{4}$$

where E_D = energy dissipated under one complete cycle by calculating the total area under the hysteresis loops using the area under the trapezium and strain energy E_{so} by calculating the area of the triangle under maximum lateral load and maximum lateral displacement. Normally, the equivalent viscous damping for the first cycle is higher than for the second cycle. Figure 7(a) shows the equivalent viscous damping of the unrepaired specimen for the first and second cycle. Meanwhile, Figure 7(b) shows the equivalent viscous damping for the repaired specimen for the first and the second cycle. The maximum equivalent

viscous damping occurring in the repaired specimen was 30%, which is due to the larger area of the hysteresis loops in the repaired specimen when compared with the unrepaired specimen. The data analysis of the results will be discussed in the next section for the second specimen, which was tested under out-of-plane lateral cyclic loading.

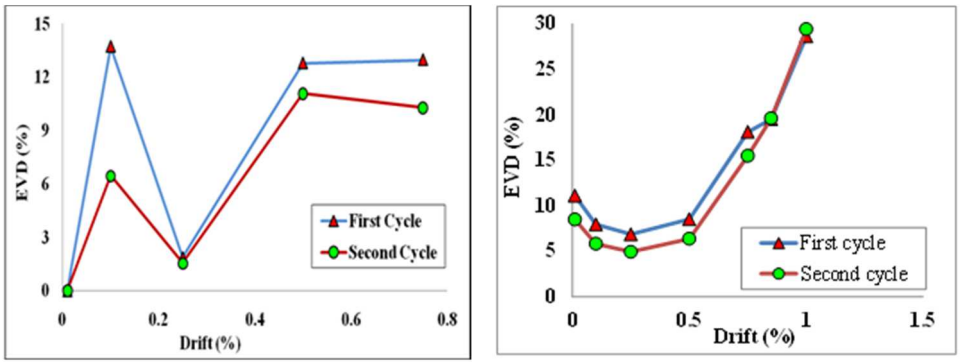

(a) EVD unrepaired specimen (b) EVD repaired specimen

Figure 7 Comparison of EVD between unrepaired and repaired specimen.

4.2 Comparison of Unrepaired and Repaired Test Model Under Out-Of-Plane Lateral Cyclic Loading

The second specimen was tested under out-of-plane lateral cyclic loading by using the drift percentages as shown in Table 1. The unrepaired specimen, which was tested under out-of-plane direction is labeled S-OUT-BR and the repaired specimen using a steel angle, a steel plate and CFRP is labeled S-OUT-AR (SA+SP+CFRP).

Figure 8 shows a comparison in terms of visually observed damage to the inner walls and wall-foundation interface of this specimen at ±1.75% drift. Figure 8(a) shows a few parallel horizontal hairline cracks on the inner shear wall at -1.75% drift. Figure 8(b) shows there were no cracks on either the outside or the inside of the wall panel at +1.75% drift. It is evident that the test model, which had been damaged after testing under out-of-plane lateral cyclic loading, performed better after being repaired with the steel angle, steel plate and CFRP. Using CFRP to wrap the damaged area can increase the confined concrete of the wall panel and prevent the wall from cracking and spalling.

Figure 9 shows a comparison of the hysteresis loops of the test model, which had been repaired and retested under out-of-plane lateral cyclic loading. The total area of the hysteresis loops for the unrepaired S-OUT-BR specimen was larger than for the S-OUT-AR(SA+SP+CFRP) repaired specimen, as shown in

Figure 9(a). However, most of the hysteresis loops from the repaired specimen shown in Figure 9(b) were very slim, where less of energy was dissipated during testing. Moreover, the highest value recorded by the load cell under out-of-plane lateral strength capacity was 8 kN, obtained from the S-OUT-AR(SA+SP+CFRP) specimen. Meanwhile, the out-of-plane lateral strength capacity of the S-OUT-BR specimen was 6 kN. Therefore, the out-of-plane lateral strength capacity was increased by 33.3% after the specimen was repaired and retrofitted using the steel plate, the steel angle and CFRP.

S-OUT-BR SPECIMEN

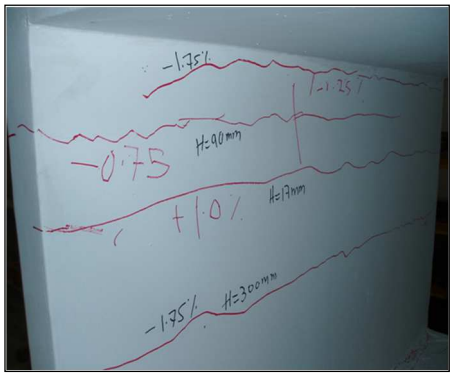

(a) Several cracks observed in the inner wall at -1.75% drift

S-OUT-AR(SA+SP+CFRP) SPECIMEN

(b) No cracks observed in the inner wall at 1.75% drift after being repaired

Figure 8 Comparison in terms of visual observation between unrepaired and repaired specimen under out-of-plane lateral cyclic loading.

S-OUT-BR SPECIMEN

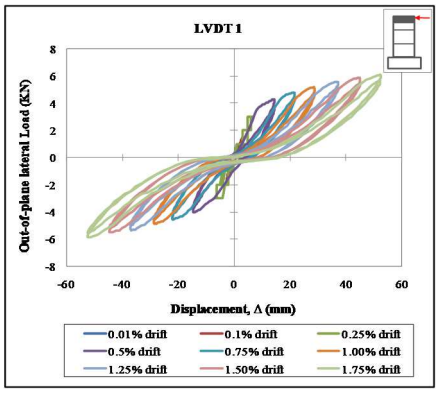

(a) Hysteresis loops at LVDT1

S-OUT-AR(SA+SP+CFRP) SPECIMEN

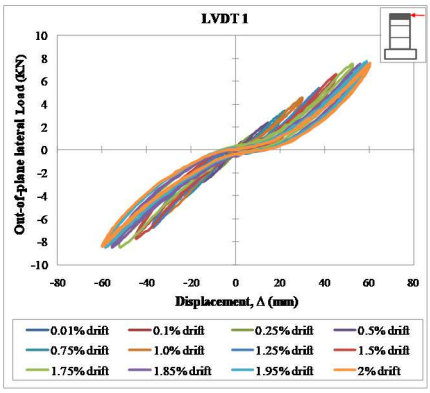

(b) Hysteresis loops at LVDT1

Figure 9 Comparison of hysteresis loops between unrepaired and repaired specimens.

The hysteresis loops of the S-OUT-BR unrepaired specimen and the S-OUT-AR(SA+SP+CFRP) unrepaired specimen shown in Figure 9 were used to calculate the seismic performance of the TFB test model under out-of-plane lateral cyclic loading. The comparison of seismic performance based on elastic stiffness (K_e), secant stiffness (K_{sec}), ductility and equivalent viscous damping was analyzed and investigated.

Table 4 shows that the maximum value for elastic stiffness was (K_e = 3.00) for the unrepaired specimen in the pushing direction of the first cycle and (K_e = 2.50) for the repaired specimen. The maximum secant stiffness of unrepaired specimen was (K_{sec} = 0.23) and (K_{sec} = 0.28) for the repaired specimen. Thus, the secant stiffness was increased significantly in the repaired specimen when compared to the unrepaired specimen.

Table 4 Values of K_e and K_{sec} of unrepaired and repaired specimens.

Stiffness (kN/mm)	**Before repair**	**After repair**	**Difference percentage**
K_e	3.00	2.50	16.67%
K_{sec}	0.17	0.26	52.94%
(a) Pushing for first cycle			
Stiffness (kN/mm)	**Before repair**	**After repair**	**Difference percentage**
K_e	0.67	0.75	11.94%
K_{sec}	0.23	0.28	21.74%
(b) Pushing for second cycle			

Table 5 shows a comparison in terms of displacement ductility between the unrepaired and the repaired specimens tested under out-of-plane lateral cyclic loading. The maximum value of displacement ductility was 2.74 as recorded in the pushing direction in the first cycle of the repaired specimen labeled as S-OUT-AR (SA+SP+CFRP). The highest difference percentage between the unrepaired and the repaired specimens occurred in the first cycle in the pushing direction (13.69%). The minimum value of displacement ductility for the unrepaired specimen was 2.38, recorded in the second cycle. These values of displacement ductility indicate that the tunnel form building system can survive under moderate to strong earthquake excitations [29].

Figure 10 shows a comparison of equivalent viscous damping (EVD) in terms of difference percentage between the unrepaired and repaired specimens. It shows that the EVD for the first cycle was always higher than for the second

cycle for both specimens, because the first cycle always required more energy to overcome the elastic strain energy before it reached the yield lateral load and yield strain. The second cycle indicates that the tunnel form building system exceeded the yield stress and yield strain of the reinforcement bars and required less energy to dissipate during testing or earthquake excitations.

Table 5 Comparison of displacement ductility between unrepaired and repaired specimens.

Cycle	Direction	Displacement ductility (μ_Δ)		Difference percentage
		S-OUT-BR	S-OUT-AR (SA+SP+CFRP)	
First cycle	Pushing	2.41	2.74	13.69%
	Pulling	2.39	2.68	12.13%
Second cycle	Pushing	2.42	2.73	12.81%
	Pulling	2.38	2.62	10.08%

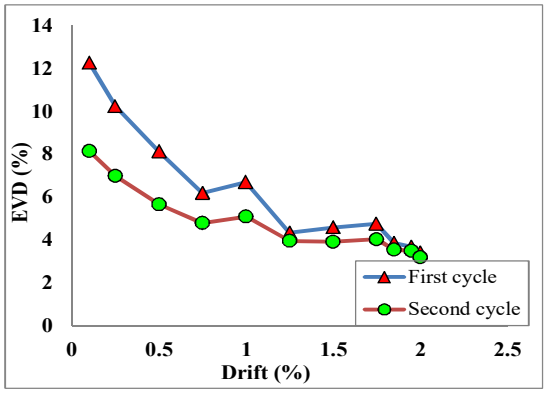

(a) EVD for S-OUT-BR specimen

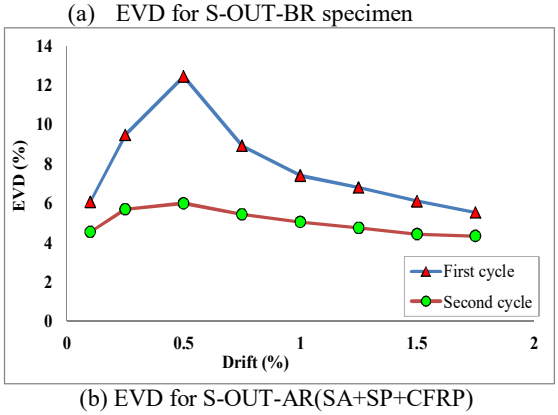

(b) EVD for S-OUT-AR(SA+SP+CFRP)

Figure 10 Comparison of equivalent viscous damping (EVD) between unrepaired and repaired specimens.

Figure 10(a) shows that the EVD for the S-OUT-BR unrepaired specimen with a maximum value of 13% occurred at 0.5% drift in the first cycle. Meanwhile, Figure 10(b) shows the EVD of the S-OUT-AR(SA+SP+CFRP) specimen with a maximum EVD of 12% occurring at 0.01% drift in the first cycle. It can be seen that the value of EVD decreased when the area of the hysteresis loops recorded at LVDT1 was very small, or vice versa. It can be concluded that the EVD for the repaired specimen became steadier when compared to the unrepaired specimen [30].

5 Conclusion and Recommendations

Seismic impacts on a test model were investigated and the optimum repair and retrofitting scheme was established to reduce the cost of repairing and retrofitting damaged buildings, to avoid demolishing buildings after an earthquake, and to reduce homelessness by re-occupying repaired buildings after a disaster. Based on the experimental work, the analysis of the results, and discussion of the two specimens, the following conclusions and recommendations can be given:

1. Based on visual observation, the repaired specimens did not suffer any cracks or spalling of the concrete when compared to the unrepaired specimens, which had horizontal cracks along the wall panel.
2. The highest value of elastic stiffness was 9.5 for the unrepaired specimen and the maximum value of secant stiffness was 1.95 for the repaired specimen tested under in-plane lateral cyclic loading. Meanwhile, maximum elastic stiffness was 3.00 for the unrepaired specimen and secant stiffness was 0.28 for the repaired specimen tested under out-of-plane lateral cyclic loading.
3. The highest value of displacement ductility was 1.54 for the repaired specimen tested under in-plane lateral cyclic loading and 2.74 for the repaired specimen under out-of-plane lateral cyclic loading.
4. The highest value of equivalent viscous damping (EVD) was 30% for the repaired specimen in the first cycle tested under in-plane lateral cyclic loading and 13% for the repaired specimen under out-of-plane lateral cyclic loading. It would be better to increase the percentage of damping rather than the stiffness of the structure because the building requires more damping in order to dissipate energy during an earthquake.
5. The optimum repair and retrofitting scheme for the damaged tunnel form building test model was the one combing a steel plate, a steel angle and CFRP.
6. It is recommended to conduct more experimental work using GFRP instead of CFRP with testing under in-plane and out-of-plane lateral cyclic loading.

Acknowledgments

Special thanks go to the e-Science Fund, Ministry of Science and Innovation (MOSTI), Putrajaya, Malaysia and RMC (Research Management Center) for funding this research work. Gratitude and appreciation go to the laboratory staff of the Faculty of Civil Engineering for their invaluable assistance during the course of this experimental research work.

References

[1] Balkaya, C. & Kalkan, E., *Nonlinear Seismic Response Evaluation of Tunnel Form Building Structures*, Computers & Structures, **81**(3), pp. 153-165, 2004a.

[2] Balkaya, C. & Kalkan, E., *Seismic Vulnerability, Behavior and Design of Tunnel Form Building Structures*, Engineering Structures, **26**(14), pp. 2081-2099, 2005b.

[3] Yuksel, S. & Kalkan, E., *Behavior of Tunnel Form Buildings under Quasi-static Cyclic Lateral Loading*, Structural Engineering and Mechanics, **27**(1), pp. 1-17, 2007.

[4] Kalkan, E. & Yuksel, S.B., *Pros and Cons of Multistory RC Tunnel-form (Box Type) Buildings*, The structural Design of Tall and Special Buildings, **26**(14), 2017.

[5] Bedirhanoglu, I., *Prefabricated-HSPRCC Panels for Retrofitting of Existing RC Members a Pioneering Study,* Structural Engineering and Mechanics, **56**(1), pp. 001-025, 2015.

[6] Boukhezar, M., Samai, M.L., Mesbah, H.A. & Houri, H., *Flexural Behavior of Reinforced Low-strength Concrete Beams Strengthened with CFRP Plates*, Structural Engineering and Mechanics, **47**(6), pp. 819-838, 2013.

[7] Balaguru, P., *FRP Composites for Reinforced and Prestressed Concrete Structures*, Taylor & Francis, 2009.

[8] Antoniades, K.K., Salonikios, T.N. & Kappos, A.J., *Tests on Seismically Damaged Reinforced Concrete Walls Repaired and Strengthened using Fiber-reinforced Polymers*, Journal of Composite for Construction, **9**(3), pp. 236-246, 2005.

[9] Ahmad, E. & Sobuz, H.R., *Experimental Study on Long-term behavior of CFRP Strengthened RC Beams under Sustained Load*, Structural Engineering and Mechanics, **40**(1), pp. 105-120, 2011.

[10] Madharan, M., Sanap, V. Verma, R. & Selvaraj, S., *Flexural Strengthening of Structural Steel Angle Sections using CFRP: Experimental Investigation*, Journal of Composite for Construction, **20**(1), 124-144, 2015.

[11] Layssi, H., Cook, W.P. & Mitchell, D., *Seismic Response and CFRP Retrofit of Poorly Detailed Shear Walls*, Journal of Composite for Construction, **16**(3), pp. 332-339, 2012.
[12] Pimanmas, A. & Thai, D.X., *Response of Lap Splice of Reinforcing Bars Confined by FRP Wrapping: Application to Nonlinear Analysis of RC Column*, Structural Engineering and Mechanics, **37**(1), pp. 111-129, 2011.
[13] Saribiyik, A. & Caglar, N., *Flexural Strengthening of RC Beams with Low-strength Concrete using GFRP and CFRP*, Structural Engineering and Mechanics, **58**(5), pp. 825-845, 2016.
[14] Ghani, K.D. & Hamid, N.H., *Experimental Investigations on a Non-seismic Precast RC Beam-column Exterior Joint Under Quasi-static Lateral Cyclic Loading*, WIT Transactions on the Built Environment, **134**, pp. 827-837, 2013.
[15] Hamid, N.H., Hadi, N.D. & Ghani, K.D., *Retrofitting of Beam-column Joint using CFRP and Steel Plate*, International Journal of Civil, Architectural Science and Engineering, **7**, pp. 542-548, 2013.
[16] Hamid, N.H., Anuar, S.H. & Azmi, N.L., *Retrofitting of a Double Unit Tunnel Form Building using Additional RC Wall, Steel Angle and CFRP*, Applied Mechanics and Materials, **661**, pp. 128-133, 2014.
[17] Tiong, P.L.Y, Adnan, A. & Hamid, N.H., *Behaviour Factor and Displacement Estimation of Low-ductility Precast Wall System under Seismic Actions*, Earthquakes and Structures, **5**(6), pp. 625-655, 2013.
[18] Woods, J., Lau, A. & Cruz-Noguez, C., *In-plane Seismic Strengthening of Nonductile Reinforced Concrete Shear Walls using Eternally Bonded CFRP Sheets*, Journal of Composite Construction, **20**(6), p. 04016052, 2016. DOI: 10.1061/(ASCE)CC.1943-5614.0000705.
[19] Chung, L. Park, T.W., & Hwang, J.H., *Strengthening Methods for Existing Wall Type Structures by Installing Additional Shear Wall*, Structural Engineering and Mechanics, **47**(4), pp. 523-536, 2014.
[20] Thermou, G. & Elnashai, A.S., *Seismic Retrofit Schemes for RC Structures and Local-global Consequences*, Earthquake Engineering and Structural Dynamics, **8**(1), pp. 1-15, 2006.
[21] Erdogan, H., Zohrevand, P. & Mirmiran, A., *Effectiveness of Externally Applied CFRP Stirrups for Rehabilitation of Slab-column Connections*, Journal of Composite for Construction, **17**(6), pp. 23-53, 2013.
[22] Kocak, A., *Earthquake Performance of FRP Retrofitting of Short Columns around Band-type Windows*, Structural Engineering and Mechanics, **53**(1), pp. 001-16, 2015.
[23] BS 8110: Part 1, *Structural Use of Concrete: Cubes, Code of Practice for Design and Construction*, British Standards Institution, UK, 1997.

[24] Abdul Ghani, K.D. & Hamid, N.H., *Comparing the Seismic Performance of Beam-Column Joints with and without SFRC when Subjected to Cyclic Loading*, Advanced Materials Research, **626**, pp. 85-89, 2013.
[25] Anudai, S., Hamid, N.H. & Hashim, M.H., *Experimental Study on Seismic Behavior of Repaired Single and Double Unit Tunnel Form Building under in Plane Cyclic Loading*, Malaysian Construction Research Journal, **17**(2), pp. 19-28, 2016.
[26] Hamid, N.H., Hadi, N.D. & Ghani, K.D., *Retrofitting of Beam-column Joint using CFRP and Steel Plate*, International Journal of Civil, Architectural Science and Engineering, **7**, pp. 542-538, 2013.
[27] Jacobsen L.S., *Steady Forced Vibrations as Influenced by Damping*. ASME Transaction, **52**(1), pp. 169-181, 1930.
[28] Chopra, A.K., *Dynamics of Structures: Theory and Application to Earthquake Engineering*, Prentice Hall, Upper Saddle River, New Jersey, United States of America, **729**, 1995.
[29] Hamid, N.H., Anuar, S.H. & Azmi, N.L., *Retrofitting of a Double Unit Tunnel Form Building using Additional RC Wall, Steel Angle and CFRP*, Advanced Mechanics and Materials, Trans Tech Publication, **661**, pp. 123-127, 2014.
[30] Anuar, S.A., Hamid, N.H., & Hashim, M.H., *Comparison of Seismic Behavior for a Single Unit Tunnel Form RC Building Before and After Repaired*, Trans Tech Publications, Advanced Materials Research, **905**, pp. 254-258, 2014.